Soft Matter

Accepted Manuscript

ROYAL SOCIETY OF CHEMISTRY

www.rsc.org/softmatter

Systematic and Simulation-Free Coarse Graining of Homopolymer Melts: A Relative-Entropy-Based Study

Delian Yang and Qiang Wang*

Department of Chemical and Biological Engineering
Colorado State University
Fort Collins, CO 80523-1370

July 13, 2015

Abstract

We applied the systematic and simulation-free strategy proposed in our previous work (D. Yang and Q. Wang, *J. Chem. Phys.*, 2015, **142**, 054905) to the relative-entropy-based (RE-based) coarse graining of homopolymer melts. RE-based coarse graining provides a quantitative measure of the coarse-graining performance and can be used to select the appropriate analytic functional forms of the pair potentials between coarse-grained (CG) segments, which are more convenient to use than the tabulated (numerical) CG potentials obtained from structure-based coarse graining. In our general coarse-graining strategy for homopolymer melts using RE framework proposed here, the bonding and non-bonded CG potentials are coupled and need to be solved simultaneously. Taking the hard-core Gaussian thread model (K. S. Schweizer and J. G. Curro, *Chem. Phys.*, 1990, **149**, 105) as the original system, we performed RE-based coarse graining using the polymer reference interaction site model theory under the assumption that the intrachain segment pair correlation

*E-mail: q.wang@colostate.edu.

functions of CG systems are the same as those in the original system, which decouples the bonding and non-bonded CG potentials and simplifies our calculations (that is, we only calculated the latter). We compared the performance of various analytic functional forms of non-bonded CG pair potential and closures for CG systems in RE-based coarse graining, as well as the structural and thermodynamic properties of original and CG systems at various coarse-graining levels. Our results obtained from RE-based coarse graining are also compared with those from structure-based coarse graining.

1 Introduction

Coarse graining of polymeric systems[1] is an active research area, because full atomistic simulations of many-chain systems used in experiments are in most cases not feasible at present due to their formidable computational requirements. Various coarse-graining methods have been proposed in the literature,[2–11] in most of which many-chain molecular simulations (i.e., molecular dynamics or Monte Carlo simulations) are used to obtain the structural and/or thermodynamic properties of both original and coarse-grained (CG) systems that need to be matched. In Ref. [12] (referred to as Paper I hereafter), we proposed a systematic and simulation-free strategy and applied it to structure-based (st-based) coarse graining of homopolymer melts, where we used integral-equation theories,[13–15] instead of many-chain simulations, to obtain the structural and thermodynamic properties of both original and CG systems, and quantitatively examined how the effective pair potentials between CG segments and the properties of CG systems vary with the coarse-graining level. Our systematic and simulation-free strategy is much faster than those using many-chain simulations, thus effectively solving the transferability problem in coarse graining,[16] and provides the quantitative basis for choosing the appropriate coarse-graining level. It also avoids the problems caused by finite-size effects and statistical uncertainties in many-chain simulations.[12]

The widely used st-based coarse graining matches the segment radial distribution functions between original and CG systems.[3–5] As expected, it cannot give the thermodynamic consistency between original and CG systems due to the information loss of coarse graining.[12,17] In this work, we apply our systematic and simulation-free strategy to the recently proposed relative-entropy-based (RE-based) coarse graining,[9,18,19] which minimizes the information loss quantified by RE. As shown by Shell, RE-based coarse graining provides a general framework and can be reduced, under further constraints, to the various coarse-graining methods previously proposed.[19] For example, when *pair* potentials are used between CG segments (which is the common practice in molecular simulations), RE-based coarse graining becomes equivalent to st-based coarse graining if the functional form of CG potentials is unconstrained (i.e., contains an infinite number of parameters).[19] It can therefore be used to parameterize CG potentials with given analytic

functional forms containing finite number of parameters, which are more convenient to use in molecular simulations than the tabulated (numerical) CG potentials obtained from st-based coarse graining. The values of minimized RE obtained from RE-based coarse graining with different CG potential functional forms can further be compared to determine the appropriate functional form or number of parameters.

To the best of our knowledge, RE-based coarse graining has not yet been applied to polymeric systems. In this work, we first describe our systematic and simulation-free strategy for RE-based coarse graining of homopolymer melts using the polymer reference interaction site model (PRISM) theory,[14] then present our numerical results with the hard-core Gaussian thread model[20] (referred to as the hard-core CGC-δ model below) solved by PRISM theory with the Percus-Yevick closure[21] as the original system, which was also used in Paper I.[12] We compare the performance of various analytic functional forms of non-bonded CG pair potential and closures for CG systems in RE-based coarse graining, as well as the structural and thermodynamic properties of original and CG systems at various coarse-graining levels. Our results obtained from RE-based coarse graining are also compared with those from st-based coarse graining presented in Paper I.[12] Finally, we elucidate in Appendix the relation between minimization of RE and the least-squares fitting of the CG potential to that obtained from st-based coarse graining.

2 Models and Methods

2.1 A general coarse-graining strategy for homopolymer melts using RE framework

We consider an original system of homopolymer melts, which consists of n chains each of N_m monomers at a chain number density $\rho_c \equiv n/V$ with V being the system volume. The invariant degree of polymerization $\bar{\mathcal{N}} \equiv (\rho_c R_{e,0}^3)^2$ controls the system fluctuations with $R_{e,0}$ being the root-mean-square end-to-end distance of an ideal chain.[22]

For coarse-graining purpose, similar to Paper I[12] we divide each original polymer

chain into N subchains (segments) each containing l consecutive monomers, such that $Nl = N_m$. Let $\mathbf{r}_{\alpha,t}$ be the spatial position of the t^{th} monomer on the α^{th} chain in the original system, and $\mathbf{R}_{\alpha,s} = \sum_{t=(s-1)l+1}^{sl} \mathbf{r}_{\alpha,t}/l$ the spatial position of the s^{th} segment (which corresponds to the center-of-mass of its monomers) on the α^{th} chain in the coarse-grained (CG) system; this defines the mapping operator $\mathbf{M}$ that gives $\mathbf{R} = \mathbf{M}(\mathbf{r})$, where $\mathbf{r}$ and $\mathbf{R}$ denote a configuration of the original system and the corresponding configuration of CG system, respectively. Furthermore, let $Z_m = \int \mathrm{d}\mathbf{r} \exp(-\beta H_m^{\text{b}} - \beta H_m^{\text{nb}})$ be the configuration integral of the original system, where $H_m^{\text{b}}(\mathbf{r})$ and $H_m^{\text{nb}}(\mathbf{r})$ are its Hamiltonian due to chain connectivity and non-bonded interactions, respectively, and $\beta \equiv 1/k_B T$ with k_B being the Boltzmann constant and T the thermodynamic temperature. Similarly, we have the configuration integral of the corresponding CG system, $Z = \int \mathrm{d}\mathbf{R} \exp(-\beta H^{\text{b}} - \beta H^{\text{nb}})$, where $H^{\text{b}}(\mathbf{R})$ and $H^{\text{nb}}(\mathbf{R})$ are its Hamiltonian due to the effective connectivity and non-bonded interactions, respectively, between CG segments.

Coarse graining using RE framework[9] minimizes RE, which can be defined as[23]

$$S \equiv -\int \mathrm{d}\mathbf{r} \mathcal{P}_m(\mathbf{r}) \ln \mathcal{P}(\mathbf{M}(\mathbf{r})) = \left\langle \beta H^{\text{b}} \right\rangle_m + \left\langle \beta H^{\text{nb}} \right\rangle_m + \ln \int \mathrm{d}\mathbf{R} \exp(-\beta H^{\text{b}} - \beta H^{\text{nb}}), \quad (1)$$

where the configurational probabilities $\mathcal{P}_m(\mathbf{r}) \equiv \exp(-\beta H_m^{\text{b}} - \beta H_m^{\text{nb}})/Z_m$ and $\mathcal{P}(\mathbf{M}(\mathbf{r})) \equiv \exp(-\beta H^{\text{b}} - \beta H^{\text{nb}})/Z$ are for the original and CG systems, respectively, and $\langle\rangle_m$ denotes the ensemble average of the original system (e.g., $\left\langle H^{\text{b}} \right\rangle_m \equiv \int \mathrm{d}\mathbf{r} \mathcal{P}_m(\mathbf{r}) H^{\text{b}}(\mathbf{M}(\mathbf{r}))$). Parameterizing the bonding and non-bonded potentials of the CG system to be dependent on $\boldsymbol{\lambda}^{\text{b}}$ and $\boldsymbol{\lambda}$, respectively, where $\boldsymbol{\lambda} = \{\lambda_j\}$ with $j = 1, \ldots, n_p$, for example, denotes the parameters to be solved and n_p the total number of these parameters, minimizing S is then equivalent to solving

$$\left\langle \frac{\partial(\beta H^{\text{b}})}{\partial \lambda_i^{\text{b}}} \right\rangle_m = \left\langle \frac{\partial(\beta H^{\text{b}})}{\partial \lambda_i^{\text{b}}} \right\rangle_{\text{CG}} \quad (2)$$

and

$$\left\langle \frac{\partial(\beta H^{\text{nb}})}{\partial \lambda_j} \right\rangle_m = \left\langle \frac{\partial(\beta H^{\text{nb}})}{\partial \lambda_j} \right\rangle_{\text{CG}} \quad (3)$$

for *all* the parameters, where the operator $\partial/\partial\lambda_j$, for example, denotes the partial derivative with respect to λ_j while keeping all other parameters constant, and $\langle\rangle_{\text{CG}}$

denotes the ensemble average of CG system. Because the ensemble averages of CG system depend on both its bonding and non-bonded potentials, $\boldsymbol{\lambda}^{\rm b}$ and $\boldsymbol{\lambda}$ are coupled and need to be solved simultaneously.

Here we consider isotropic pair potentials for the effective interactions in the CG system. In particular, its bonding Hamiltonian is given by $\beta H^{\rm b} = \sum_{\alpha=1}^{n}\sum_{k=1}^{K}\sum_{s=1}^{N-k}\beta v_k^{\rm b}(|\mathbf{R}_{\alpha,s+k}-\mathbf{R}_{\alpha,s}|;\boldsymbol{\lambda}_k^{\rm b})$, where $\beta v_k^{\rm b}(r)$ is the bonding potential acting on two segments with $k-1$ segments between them (excluding the two segments) on the same chain and is parameterized by a set of parameters $\boldsymbol{\lambda}_k^{\rm b}$ (i.e., $\boldsymbol{\lambda}^{\rm b}=\{\boldsymbol{\lambda}_k^{\rm b}\}$ with $k=1,\ldots,K<N$), and its non-bonded Hamiltonian is given by $\beta H^{\rm nb} = \left[\sum_{\alpha=1}^{n}\sum_{\alpha'=1}^{n}\sum_{s=1}^{N}\sum_{s'=1}^{N}\beta v(|\mathbf{R}_{\alpha,s}-\mathbf{R}_{\alpha',s'}|;\boldsymbol{\lambda}) - nN\beta v(0;\boldsymbol{\lambda})\right]\Big/2$, where $\beta v(r)$ is the non-bonded potential between two segments and is parameterized by $\boldsymbol{\lambda}$. Eqs. (2) and (3) then become

$$\sum_{s=1}^{N-k}\int_0^\infty {\rm d}r\left[\omega_{s,s+k}^{ss}(r)-\omega_{s,s+k}(r;\boldsymbol{\lambda}^{\rm b},\boldsymbol{\lambda})\right]r^2\frac{\partial\beta v_k^{\rm b}(r)}{\partial\lambda_{k,i}^{\rm b}}=0 \qquad (k=1,\ldots,K) \tag{4}$$

and

$$\sum_{s=1}^{N}\sum_{s'=1}^{N}\int_0^\infty {\rm d}r\,\frac{r^2}{R_{e,0}^3}\left\{R_{e,0}^3\left[\omega_{s,s'}^{ss}(r)-\omega_{s,s'}(r;\boldsymbol{\lambda}^{\rm b},\boldsymbol{\lambda})\right]+\sqrt{\mathcal{N}}\left[g_{s,s'}^{ss}(r)-g_{s,s'}(r;\boldsymbol{\lambda}^{\rm b},\boldsymbol{\lambda})\right]\right\} \times\frac{\partial\beta v(r)}{\partial\lambda_j}=0, \tag{5}$$

respectively, where $\omega_{s,s'}^{ss}(r)$ and $g_{s,s'}^{ss}(r)$ are the normalized (i.e., $4\pi\int_0^\infty {\rm d}r r^2\omega_{s,s'}^{ss}(r)=1$) intrachain pair correlation function (PCF) and the interchain radial distribution function, respectively, between segments s and s' in the space of $\mathbf{M}(\mathbf{r})$ in the original system (denoted by the superscript "ss"), and $\omega_{s,s'}(r)$ and $g_{s,s'}(r)$ are the normalized intrachain PCF and the interchain radial distribution function, respectively, between segments s and s' in the CG system. Note that $\omega_{s,s'}(r)$ and $g_{s,s'}(r)$ depend on all $\beta v_k^{\rm b}(r)$ (thus $\boldsymbol{\lambda}^{\rm b}$) and $\beta v(r)$ (thus $\boldsymbol{\lambda}$), while $\omega_{s,s'}^{ss}(r)$ and $g_{s,s'}^{ss}(r)$ do not; in particular, many-chain molecular simulations or the self-consistent integral-equation theories[24,25] of the CG system are needed to obtain $\omega_{s,s'}(r;\boldsymbol{\lambda}^{\rm b},\boldsymbol{\lambda})$.

Finally, neglecting the chain-end effects, i.e., assuming that both $\omega^{ss}_{s,s'}(r)$ and $\omega_{s,s'}(r)$ depend only on $|s-s'|$, $g^{ss}_{s,s'}(r) = g^{ss}(r)$, and $g_{s,s'}(r) = g(r)$ for all s and s', we can simplify Eqs. (4) and (5) as

$$\int_0^\infty \mathrm{d}r \left[\omega^{ss}_{1,k+1}(r) - \omega_{1,k+1}(r;\boldsymbol{\lambda}^{\mathrm{b}},\boldsymbol{\lambda})\right] r^2 \frac{\partial \beta v^{\mathrm{b}}_k(r)}{\partial \lambda^{\mathrm{b}}_{k,i}} = 0 \qquad (k = 1,\ldots,K) \tag{6}$$

and

$$\int_0^\infty \mathrm{d}r \frac{r^2}{R^3_{e,0}} \left\{ R^3_{e,0} \left[\omega^{ss}(r) - \omega(r;\boldsymbol{\lambda}^{\mathrm{b}},\boldsymbol{\lambda})\right] + \sqrt{\bar{\mathcal{N}}} \left[g^{ss}(r) - g(r;\boldsymbol{\lambda}^{\mathrm{b}},\boldsymbol{\lambda})\right] \right\} \frac{\partial \beta v(r)}{\partial \lambda_j} = 0, \tag{7}$$

respectively, where $\omega^{ss}(r) \equiv \sum_{s=1}^N \sum_{s'=1}^N \omega^{ss}_{s,s'}(r)/N^2$ and $\omega(r) \equiv \sum_{s=1}^N \sum_{s'=1}^N \omega_{s,s'}(r)/N^2$. Eqs. (6) and (7) are for RE-based coarse graining of homopolymer melts and can be compared with st-based coarse graining, which gives $\omega_{s,s'}(r) = \omega^{ss}_{s,s'}(r)$ and $g(r) = g^{ss}(r)$ at *all* r by adjusting an *infinite* number of parameters.

2.2 Coarse graining of hard-core CGC-δ model using PRISM theory

To demonstrate our general coarse-graining strategy described above, as in Paper I[12] we take the hard-core CGC-δ model[20] as the original system, which consists of continuous Gaussian chains each of $N_m \to \infty$ monomers interacting with the non-bonded pair potential $\beta u_m(r) = (\bar{\kappa}/\rho_c N_m^2)\delta(r)$ with $\bar{\kappa} \to \infty$. This simple model system is solved using PRISM theory with the Percus-Yevick (PY) closure[21] and ideal-chain conformations, which then results in $\omega^{ss}_{s,s'}(r)$ and $g^{ss}(r)$ for given N according to Eqs. (A11) and (19) in Paper I,[12] respectively, as well as its structural and thermodynamic properties; for more details, we refer the readers to Paper I.[12] Note that, to simplify our calculations by avoiding the aforementioned many-chain simulations or the self-consistent integral-equation theories[24,25] of the CG system, in this work we assume $\omega_{s,s'}(r) = \omega^{ss}_{s,s'}(r)$, which de-couples $\boldsymbol{\lambda}^{\mathrm{b}}$ and $\boldsymbol{\lambda}$; in other words, we only solve $\beta v(r)$ (i.e., $\boldsymbol{\lambda}$) from Eq. (7), which now becomes

$$\int_0^\infty \mathrm{d}r \frac{r^2}{R^3_{e,0}} \left[g^{ss}(r) - g(r;\boldsymbol{\lambda})\right] \frac{\partial \beta v(r)}{\partial \lambda_j} = 0 \qquad (j = 1,\ldots,n_p). \tag{8}$$

For the CG system at given N, PRISM theory gives

$$\hat{h} = N^2 \hat{\omega} \hat{c} (\hat{\omega} + \rho_c \hat{h}), \tag{9}$$

where $h(r) \equiv g(r) - 1$ and $c(r)$ are the interchain total and direct PCFs between CG segments, respectively, and we use the short-hand notation $\hat{f} = (4\pi/q) \int_0^\infty \mathrm{d}r f(r) r \sin(qr)$ to denote the 3D Fourier transform of a radial function $f(r)$ with q being the wavevector length. With $\omega(r) = \omega^{ss}(r)$ given by the our assumption above, we numerically solve Eq. (9) for given $\beta v(r; \boldsymbol{\lambda})$ with various closures, written in general as

$$c(r) = \exp[-\beta v(r) + \gamma(r) + b(r)] - [\gamma(r) + 1], \tag{10}$$

where $\gamma(r) \equiv h(r) - c(r)$ is the interchain indirect PCF and $b(r)$ the bridge function. In particular, we consider three commonly used closures in this work: $b(r) = 0$ for the hypernetted-chain (HNC) closure,[26] $\ln[\gamma(r) + 1] - \gamma(r)$ for PY closure,[21] and $\ln[h(r) + 1] - h(r)$ for the random-phase approximation (RPA) closure;[27] for the relation among these closures, we refer the readers to Paper I.[12]

Note that RPA closure can be written as $c(r) = -\beta v(r)$, which directly leads to $c(r)$ for given $\beta v(r; \boldsymbol{\lambda})$. On the other hand, to solve Eq. (9) with HNC and PY closures, we first re-write it as

$$\hat{\gamma} = \hat{\omega}^2 \hat{c} / (N^{-2} - \rho_c \hat{\omega} \hat{c}) - \hat{c}, \tag{11}$$

from which we obtain $\hat{\gamma}$ (and thus $\gamma(r)$) for given $c(r)$. We then obtain the new direct PCF from Eq. (10), and use the Anderson mixing method[28,29] to converge $c(r)$ till the maximum absolute residual error of Eq. (10) at all r is less than 10^{-14}. Note that $c(r)$ approaches 0 when r is on the order of the interaction range of βv, while $h(r)$ (and $\gamma(r)$) approaches 0 when r is on the order of $R_{e,0}$. We therefore use a cut-off length $r_c = 30 R_{e,0}$ for $h(r)$ with $[0, r_c]$ uniformly discretized into 3×10^4 subintervals, and a cut-off length of $r_c/\sqrt{N}$ for $c(r)$; our cut-off and discretization give negligible numerical errors. We also use FFTW[30] to perform the Fourier transforms of PCFs with the above cut-off and discretization, where r_c determines the discretization of q-space and the subinterval size determines the cut-off in q-space.

Finally, we use the Newton's method combined with a globally convergent strategy[31] to solve for $\boldsymbol{\lambda}$ from Eq. (8) till the maximum absolute value of its left-hand-side is smaller than 10^{-12}, where the Romberg integration[31] is used to evaluate the integral with the cut-off r_c. We then calculate the minimized RE, as well as the structural and thermodynamic properties of the CG system at given N (see Sec. 2.4 below).

2.3 Parameterization of CG pair potential

In this work, we take the functional form of $\beta v(r)$ as suggested by the effective pair potential between CG segments $\beta v^{\rm st}(r)$ obtained from our st-based coarse graining reported in Paper I.[12] As shown there, $\beta v^{\rm st}(r)$ can be approximated by a Gaussian function at small r (where $\beta v^{\rm st}(r) > 0$). Our first way of parameterizing $\beta v(r)$ is therefore to represent it as a summation of $n_{\rm G}$ Gaussian functions, i.e.,

$$\beta v_{{\rm I},n_{\rm G}}(r;\boldsymbol{\lambda}) = \sum_{i=1}^{n_{\rm G}} A_i \exp\left(-B_i \tilde{r}^2\right) \tag{12}$$

with $n_p = 2n_{\rm G}$ parameters $A_i > 0$ and $B_i > 0$ ($i = 1, ..., n_{\rm G}$), where $\tilde{r} \equiv N^{3/4} r/R_{e,0}$ is used to take into account the $N^{-3/4}$ scaling of the CG potential range found in Refs. [12,32].

On the other hand, $\beta v_{{\rm I},n_{\rm G}}(r;\boldsymbol{\lambda})$ cannot capture the attractive well of $\beta v^{\rm st}(r) < 0$ at large $\tilde{r}$, which has significant effects on both structural and thermodynamic properties of CG systems, especially at small N, as shown in Secs. 3.1 and 3.3 below. We therefore propose another way of parameterizing $\beta v(r)$ as

$$\beta v_{\rm II}(r;\boldsymbol{\lambda}) = A \exp\left(-B\tilde{r}^2\right) W(\tilde{r}) + C \frac{\sin(D\tilde{r})}{D\tilde{r}} \exp(-E\tilde{r}) \left[1 - W(\tilde{r})\right], \tag{13}$$

where the weighting function $W(\tilde{r}) = \exp(-F\tilde{r}^2)$ is used to combine the two terms on the right-hand-side of Eq. (13) dominating at small and large $\tilde{r}$, respectively. This leads to $n_p = 6$ parameters: A, B, C, D, E, and F, all of which are positive.

2.4 Calculation of structural and thermodynamic properties of CG systems and the minimized RE using PRISM theory

Once the optimized pair potential $\beta v(r)$ is obtained for the CG system at given N, its normalized isothermal compressibility[12] is calculated as $\kappa_T = 1 + \sqrt{\bar{\mathcal{N}}}\hat{h}(0)/R_{e,0}^3$, where $\hat{h}(0)$ is solved from Eq. (9) with a closure, and its interchain internal energy per chain and interchain virial pressure are calculated as

$$\beta u_c = 2\pi N^2 \sqrt{\bar{\mathcal{N}}} \int_0^\infty \mathrm{d}r \frac{r^2}{R_{e,0}^3} g(r)\beta v(r), \tag{14}$$

$$\beta R_{e,0}^3 P = -\frac{2\pi N^2 \bar{\mathcal{N}}}{3} \int_0^\infty \mathrm{d}r \frac{r^2}{R_{e,0}^3} g(r) \frac{\mathrm{d}\beta v(r)}{\mathrm{d}\ln r}, \tag{15}$$

respectively, where the integrals are numerically evaluated using Romberg integration[31] with the aforementioned cut-off and discretization.

In general, the minimized RE per chain can be written as $s_c \equiv S/n = \left\langle \beta H^{\mathrm{b}} + \beta H^{\mathrm{nb}} \right\rangle_m / n - \beta \Delta f_c$, where Δf_c denotes the difference in the Helmholtz free energy per chain of the CG system (where $\epsilon^{\mathrm{b}} = \epsilon = 1$) from the reference state of an ideal gas of CG segments (where $\epsilon^{\mathrm{b}} = \epsilon = 0$) and can be calculated via thermodynamic integration (over $\epsilon^{\mathrm{b}} = 0 \sim 1$ at $\epsilon = 0$ and then over $\epsilon = 0 \sim 1$ at $\epsilon^{\mathrm{b}} = 1$); we therefore have

$$\begin{aligned} s_c = {} & 4\pi \sum_{k=1}^{K} (N-k) \int_0^\infty \mathrm{d}r \left[\omega_{1,k+1}^{ss}(r) - \int_0^1 \mathrm{d}\epsilon^{\mathrm{b}} \omega_{1,k+1}(r; \epsilon^{\mathrm{b}}, \epsilon = 0) \right] \beta v_k^{\mathrm{b}}(r) \\ & + 2\pi N^2 \int_0^\infty \mathrm{d}r \frac{r^2}{R_{e,0}^3} \left\{ R_{e,0}^3 \left[\omega^{ss}(r) - \int_0^1 \mathrm{d}\epsilon \omega(r; \epsilon^{\mathrm{b}} = 1, \epsilon) \right] \right. \\ & \left. + \sqrt{\bar{\mathcal{N}}} \left[g^{ss}(r) - \int_0^1 \mathrm{d}\epsilon g(r; \epsilon^{\mathrm{b}} = 1, \epsilon) \right] \right\} \beta v(r), \end{aligned} \tag{16}$$

where $\omega(r; \epsilon^{\mathrm{b}}, \epsilon)$ and $g(r; \epsilon^{\mathrm{b}}, \epsilon)$ are, respectively, the intrachain and interchain segment radial distribution functions of the CG system with the bonding potentials $\epsilon^{\mathrm{b}} v_k^{\mathrm{b}}(r)$ (after $\beta v_k^{\mathrm{b}}(r)$ for $k = 1, \ldots, K$ are obtained from the RE minimization) and the non-bonded potential $\epsilon v(r)$.

In this work, our assumption of $\omega_{s,s'}(r) = \omega^{ss}_{s,s'}(r)$ reduces Eq. (16) to

$$s_c = 2\pi N^2 \int_0^\infty \mathrm{d}r \frac{r^2}{R^3_{e,0}} \left\{ \sqrt{\bar{\mathcal{N}}} \left[g^{ss}(r) - \int_0^1 \mathrm{d}\epsilon g(r;\epsilon) \right] \right\} \beta v(r), \tag{17}$$

and we obtain $g(r;\epsilon)$ from PRISM theory with a closure. We use Romberg integration[31] to evaluate the integrals, where the cut-off r_c is used for the integration over r, and uniformly discretize the integration over ϵ into enough subintervals so that the accuracy of calculated s_c is on the order of 10^{-7} (for $N = 1$) to 10^{-5} (for $N = 100$). s_c provides a quantitative measure of the overall quality of coarse graining,[19] and can be compared for various closures of CG systems and various ways of parameterizing $\beta v(r)$. Finally, we note that Eq. (17), with $g(r;\epsilon)$ calculated at $\epsilon v^{\mathrm{st}}(r)$ and $v(r)$ replaced by $v^{\mathrm{st}}(r)$, can also be used to calculate s_c for our st-based coarse graining reported in Paper I.[12]

3 Results and Discussions

In this work we set $\bar{\mathcal{N}} = 10^4$; other values of $\bar{\mathcal{N}}$ do not qualitatively change our results. We examine first in Sec. 3.1 the non-bonded CG pair potential $\beta v(r)$ obtained from RE-based coarse graining with various closures and parameterization, then in Sec. 3.2 the minimized RE, and finally in Sec. 3.3 the structural and thermodynamic properties of CG systems. Our results obtained from RE-based coarse graining are also compared with those from st-based coarse graining.[12]

3.1 CG potentials

Our results of st-based coarse graining were presented in detail in Paper I, so here we mainly focus on the difference between $\beta v(r)$ and the CG pair potential $\beta v^{\mathrm{st}}(r)$ from st-based coarse graining, both obtained at the same N and with the same closure for the CG system. Fig. 1(a) shows the CG potentials obtained with HNC closure, where various N and parameterization of $\beta v(r)$ are used. We see that $\beta v_{\mathrm{I},2}(r)$ is overall smaller than $\beta v^{\mathrm{st}}(r)$, especially at small N; note that $\beta v_{\mathrm{I},1}(r)$ is even much smaller than $\beta v_{\mathrm{I},2}(r)$ (data not shown). We attribute this mainly to the absence of the attractive well in $\beta v_{\mathrm{I}}(r)$. As

N increases, $\beta v_{\rm I}(r)$ approaches $\beta v^{\rm st}(r)$ because the attractive well of $\beta v^{\rm st}(r)$ becomes relatively (compared to $\beta v^{\rm st}(r=0)$) small as shown in Figs. 4 and 5 of Paper I.[12] $\beta v_{\rm II}(r)$, on the other hand, is much closer to $\beta v^{\rm st}(r)$ than $\beta v_{\rm I}(r)$. As shown in Fig. 1(a), $\beta v_{\rm II}(r)$ and $\beta v^{\rm st}(r)$ are almost indistinguishable at small N; as N increases, $\beta v_{\rm II}(r)$ slightly deviates from $\beta v^{\rm st}(r)$ at small $\tilde{r}$. Note that $\beta v_{\rm II}(r)$ can well capture the attractive well of $\beta v^{\rm st}(r)$ as shown in the inset of Fig. 1(a), although the attractive well of $\beta v_{\rm II}(r)$ is shallower than that of $\beta v^{\rm st}(r)$.

To highlight the importance of the attractive well, which occurs at large r and cannot be captured by $\beta v_{\rm I}(r)$, we note that Eq. (14) can be re-written as

$$\beta u_c = 2\pi\sqrt{\bar{\mathcal{N}}}\int_0^\infty {\rm d}\tilde{r}\frac{\tilde{r}^2\beta v(\tilde{r})}{N^{1/4}}g(\tilde{r}), \tag{18}$$

which indicates that it is $\tilde{r}^2\beta v(\tilde{r})$ that determines the internal energy; similarly, Eq. (15) can be re-written as

$$\beta R_{e,0}^3 P = -\frac{2\pi\bar{\mathcal{N}}}{3}\int_0^\infty {\rm d}\tilde{r}\frac{\tilde{r}^3}{N^{1/4}}\frac{{\rm d}\beta v(\tilde{r})}{{\rm d}\tilde{r}}g(\tilde{r}), \tag{19}$$

which indicates that it is $\tilde{r}^3({\rm d}\beta v/{\rm d}\tilde{r})$ that determines the pressure. In accordance with Fig. 1(a), Figs. 1(b) and 1(c) show $\tilde{r}^2\beta v(\tilde{r})/N^{1/4}$ and $-\tilde{r}^3({\rm d}\beta v/{\rm d}\tilde{r})/N^{1/4}$, respectively, which exhibit qualitatively the same behavior. Quantitatively, however, the attractive well is shifted to larger $\tilde{r}$ in Fig. 1(c) and thus more important in determining the pressure than the internal energy. We therefore clearly see that the seemingly negligible attractive well in Fig. 1(a) is actually needed for closely reproducing the thermodynamic properties of the original system; this is supported by our results shown in Sec. 3.3 below. We also note that similar results are found for RPA and PY closures for CG systems (data not shown).

To quantify the deviation between $\beta v^{\rm st}(r)$ and $\beta v(r)$ obtained at given N, we define $\chi_v^2 \equiv (4\pi/R_{e,0}^3)\int_0^\infty {\rm d}r r^2[\beta v^{\rm st}(r) - \beta v(r)]^2$. Fig. 1(d) shows χ_v^2 vs. N for various parameterization of $\beta v(r)$ obtained with HNC closure. Consistent with Fig. 1(a), we see that χ_v^2 decreases with increasing n_p and with increasing N (except for $\beta v_{\rm II}(r)$ at

$N \geq 59$). Similar results are found for RPA and PY closures (data not shown).

Fig. 1(e) shows $\beta v(r = 0)$ as a function of N for st- and RE-based coarse graining obtained with HNC and RPA closures. In all cases, we see that the corresponding HNC and RPA results are close at small N but deviate at large N. In particular, while all HNC results of $\beta v(r = 0)$ monotonically increase with increasing N as expected (the same is found for PY results; data not shown), all RPA results of $\beta v(r = 0)$ exhibit a maximum around $N = 40$, indicating the qualitative failure of RPA closure for CG systems at larger N; for st-based coarse graining this failure was explained in Sec. IVA of Paper I,[12] and the same reason holds for RE-based coarse graining.

For both HNC and RPA closures, we see that $\beta v^{\rm st}(r = 0)$ is the largest and that $\beta v_{\rm II}(r = 0)$ is only slightly smaller than $\beta v^{\rm st}(r = 0)$ with $\beta v^{\rm st}(r = 0) - \beta v_{\rm II}(r = 0)$ monotonically increasing with increasing N. In particular, both $\beta v_{\rm II}(r = 0)$ and $\beta v^{\rm st}(r = 0)$ obtained from HNC closure scale approximately with $N^{0.18}$. $\beta v_{\rm I,2}(r = 0)$, however, is significantly different from (smaller than) $\beta v^{\rm st}(r = 0)$ at small $N \lesssim 10$; as N increases, $\beta v^{\rm st}(r = 0) - \beta v_{\rm I,2}(r = 0)$ monotonically decreases for RPA closure but exhibits a minimum at $N = 27$ for HNC closure. While $\beta v_{\rm II}(r = 0)$ is always larger (i.e., closer to $\beta v^{\rm st}(r = 0)$) than $\beta v_{\rm I,2}(r = 0)$ for HNC closure, they cross around $N = 20$ for RPA closure. Our PY results (data not shown) are qualitatively similar to HNC results. We conclude that $\beta v_{\rm II}(r)$ is a better choice for parameterizing $\beta v^{\rm st}(r)$, which has a non-trivial attractive well, and that the absence of this attractive well in $\beta v_{\rm I}$ deceases $\beta v_{\rm I}(r = 0)$ (and also $\beta v_{\rm I}(r)$ at small $\tilde{r}$) even at $N = 100$.

As shown in Figs. 5(c) and 5(d) of Paper I,[12] $\tilde{v}^{\rm st}(r) \equiv v^{\rm st}(r)/v^{\rm st}(r = 0)$ for various N collapse approximately onto the same curve, if r is normalized by $R_{e,0}N^k$ with $k \approx -0.73$ at $\bar{\mathcal{N}} = 10^4$; note that k approaches $-3/4$ as $\bar{\mathcal{N}} \to \infty$.[12,32] Fig. 2(a) shows that $\tilde{v}_{\rm II}(r)$ obtained with HNC closure also exhibits the same behavior, where $k = -3/4$ is used. The inset of Fig. 2(a) shows that the attractive well is approximately located around $\tilde{r} = 5$.

Since $\tilde{v}_{\rm II}(r)$ for various N approximately collapse, we expect a rather weak N-dependence

of all parameters in the functional form of $\beta v_{\rm II}(r)$; this is examined in Fig. 2(b). Writing $\tilde{v}_{\rm II}(r) = \exp[-(B+F)\tilde{r}^2] + (C/A)[\sin(D\tilde{r})/D\tilde{r}]\exp(-E\tilde{r})[1-\exp(-F\tilde{r}^2)]$, we see that the parameters C/A, E and D are indeed weakly dependent on N, but B and F have much stronger dependence. Note that the large value of $B+F$ makes the first term of $\tilde{v}_{\rm II}(r)$ decay very fast with $\tilde{r}$; in other words, this term only affects $\tilde{v}_{\rm II}(r)$ at small $\tilde{r}$. Similarly, the term $1-\exp(-F\tilde{r}^2)$ is approximately 1 at large $\tilde{r}$ because of the large value of F. This explains why $\tilde{v}_{\rm II}(r)$ is more collapsed at large $\tilde{r}$ than at small $\tilde{r}$ as shown in Fig. 2(a). In addition, since the large value of $B+F$ makes the first term of $\tilde{v}_{\rm II}(r)$ negligible at large $\tilde{r}$, π/D approximately gives the first root $\tilde{r}_1$, at which $\tilde{v}_{\rm II}(r)=0$; our numerical results give the average value (over $3 \le N \le 100$) of $D \approx 0.69$ and thus $\tilde{r}_1 \approx 4.53$, consistent with the inset of Fig. 2(a). We also note that $C/A > 1$; the second term in $\beta v_{\rm II}$ (thus the attractive well) is therefore significant. Finally, similar results are found for RPA and PY closures (data not shown).

3.2 Relative entropy

Fig. 3(a) compares RE per chain $s_c^{\rm st}$ for st-based coarse graining with various closures for CG systems. Note that, in the calculation of s_c, we do not consider the contribution from the mapping entropy defined in Ref. [19], which is independent of CG potential; this contribution stems from the degeneracy of different original configurations that map to the same CG configuration and should decrease with increasing N. We see that $s_c^{\rm st}$ decreases with increasing N for all closures, which is also the case when this contribution is included; in other words, the information loss due to coarse graining decreases with increasing N, which is well expected.

We also find that $s_c^{\rm st}$ obtained from HNC and RPA closures, denoted by $s_{c,\rm HNC}^{\rm st}$ and $s_{c,\rm RPA}^{\rm st}$, respectively, are nearly indistinguishable at small N. Furthermore, $s_{c,\rm HNC}^{\rm st}$ is always smaller than both $s_{c,\rm RPA}^{\rm st}$ and $s_{c,\rm PY}^{\rm st}$, and $s_{c,\rm RPA}^{\rm st} < s_{c,\rm PY}^{\rm st}$ for $N \le 26$ and the opposite occurs for larger N. Compared to Fig. 6 in Paper I,[12] we see that the information loss due to coarse graining quantified by $s_c^{\rm st}$ is qualitatively consistent with the deviation in thermodynamic properties between original and CG systems; that is, for both the interchain internal energy per chain and the interchain virial pressure of CG systems,

HNC results are always closer to the original system (i.e., better) than RPA and PY results, and RPA results are better than PY results for small N and the opposite occurs for large N. Note that, because RPA closure for CG systems qualitatively fails for large $N \gtrsim 40$ as shown in Fig. 3(a) of Paper I[12] and in Fig. 1(e), hereafter we focus only on the results obtained with HNC closure for CG systems.

Fig. 3(b) compares s_c between st- and RE-based coarse graining with various CG potential parameterization for the latter. We see that the difference in s_c between these two coarse-graining methods $s_c^{\mathrm{RE}} - s_c^{\mathrm{st}} > 0$ in all cases; in other words, st-based coarse graining gives less information loss than RE-based coarse graining at the same N. This is expected according to Ref. [19], where it was shown that st-based coarse graining is equivalent to RE-based coarse graining with an infinite number of parameters in $\beta v(r)$. We also find in Fig. 3(b) that s_c^{RE} decreases with increasing N, by noting the variation of s_c^{st} (from 0 to -20 as shown in Fig. 3(a)) and that of $s_c^{\mathrm{RE}} - s_c^{\mathrm{st}}$ (from 0 to 0.5) for $1 \leq N \leq 100$.

Our st-based coarse-graining results reported in Paper I[12] suggest that CG potentials can be approximated by a Gaussian function. Fig. 3(b) shows that using two Gaussian functions (i.e., $\beta v_{\mathrm{I},2}(r)$) gives much less information loss than using just one (i.e., $\beta v_{\mathrm{I},1}(r)$). Furthermore, our results in Paper I[12] show that $\beta v^{\mathrm{st}}(r)$ exhibits an attractive well (i.e., $\beta v^{\mathrm{st}}(r) < 0$) at large $\tilde{r} \approx 5$, which has significant effects on both structural and thermodynamic properties of CG systems, and Fig. 3(b) shows that capturing this attractive well with the second term in Eq. (13) (i.e., $\beta v_{\mathrm{II}}(r)$) gives even better coarse-graining performance. Finally, Fig. 3(b) shows that $s_c^{\mathrm{RE}} - s_c^{\mathrm{st}}$ increases with increasing N. In particular, $\beta v_{\mathrm{II}}(r)$ gives the smallest $s_c^{\mathrm{RE}} - s_c^{\mathrm{st}} < 3 \times 10^{-4}$ and is therefore good enough to analytically represent $\beta v^{\mathrm{st}}(r)$ in the N-range considered in this paper.

3.3 Structural and thermodynamic properties

In this section we compare the normalized isothermal compressibility κ_T and the interchain virial pressure $\beta R_{e,0}^3 P$ between st- and RE-based coarse graining with HNC closure for CG systems; the behavior of interchain internal energy per chain is similar to

that of the pressure and thus not shown. Note that the st-based result $\kappa_T^{\rm st}$ is the same as that of the original system and is independent of N, and that we refer the readers to Paper I[12] for the calculation of these thermodynamic properties of CG systems in st-based coarse graining.

As aforementioned, RE-based coarse graining using $\beta v_{\rm I,1}(r)$ gives poor performance. This is also shown in Fig. 4(a), where we see that κ_T obtained using $\beta v_{\rm I,1}(r)$ is significantly larger than $\kappa_T^{\rm st}$. κ_T obtained using $\beta v_{\rm I,2}(r)$ is closer to $\kappa_T^{\rm st}$ but still overestimates it for small $N \lesssim 10$. The poor performance of $\beta v_{\rm I}(r)$ is again due to the absence of the attractive well in its functional form. On the other hand, using $\beta v_{\rm II}(r)$ gives better results than using $\beta v_{\rm I}(r)$, although $\kappa_T^{\rm st}$ is somewhat underestimated for small $N \lesssim 10$.

Fig. 4(b) shows that using $\beta v_{\rm I,2}(r)$ always underestimates the pressure of the original system, P_m, particularly for $N \lesssim 30$, again due to the absence of the attractive well. Using $\beta v_{\rm I,1}(r)$ gives even smaller P (data not shown). Note, however, that the results for $27 \leq N \leq 91$ obtained from RE-based coarse graining using $\beta v_{\rm I,2}(r)$ are closer to P_m than the corresponding st-based results. On the other hand, using $\beta v_{\rm II}(r)$ gives better results than using $\beta v_{\rm I,2}(r)$ at small N. Unlike using $\beta v_{\rm I,2}(r)$, however, using $\beta v_{\rm II}(r)$ overestimates P_m for $N \lesssim 30$. Finally, Fig. 4(b) also shows that using $\beta v_{\rm I,2}(r)$ gives closer prediction of $\beta R_{e,0}^3 P$ to the original system than using $\beta v_{\rm II}(r)$ for $N \geq 36$, although the latter gives smaller $s_c^{\rm RE}$ as shown in Fig. 3(b). Minimizing RE is therefore not equivalent to matching structural or thermodynamic properties between the original and CG systems. Similarly, in Appendix we show the relation (difference) between RE minimization and the least-squares fitting of $\beta v(r)$ to $\beta v^{\rm st}(r)$.

4 Conclusions

In Ref. [12] (referred to as Paper I), we proposed a systematic and simulation-free strategy for coarse graining of polymer melts, where we used integral-equation theories,[13–15] instead of many-chain molecular simulations, to obtain the structural and thermodynamic properties of both original and coarse-grained (CG) systems, and quantitatively examined

how the pair potentials between CG segments and the thermodynamic properties of CG systems vary with the number of CG segments per chain N. We applied our strategy to structure-based (st-based) coarse graining in Ref. [12], which matches the structural correlations of CG segments between original and CG systems. In this work, we have applied it to the relative-entropy-based (RE-based) coarse graining,[9,18,19] which provides a quantitative measure of the coarse-graining performance and can be used to select the appropriate analytic functional forms of the CG potentials. Such analytic forms are more convenient to use than the tabulated (numerical) CG potentials obtained from st-based coarse graining.

We have first proposed in Sec. 2.1 a general coarse-graining strategy for homopolymer melts using RE framework, where the bonding and non-bonded CG potentials are coupled and need to be solved simultaneously. Taking the hard-core Gaussian thread model[20] (referred to as the hard-core CGC-δ model) solved by the polymer reference interaction site model (PRISM) theory[14] with the Percus-Yevick (PY) closure[21] as the original system, which was also used in Paper I,[12] we have then performed RE-based coarse graining under the assumption that the intrachain segment pair correlation functions of CG systems are the same as those in the original system (i.e., $\omega_{s,s'}(r) = \omega^{ss}_{s,s'}(r)$), which de-couples the bonding and non-bonded CG potentials and simplifies our calculations (that is, we have only calculated the latter). We have used three functional forms of the non-bonded CG pair potential $\beta v(r)$ [i.e., $\beta v_{\rm I,1}(r)$, $\beta v_{\rm I,2}(r)$, and $\beta v_{\rm II}(r)$ given by Eqs. (12) and (13), which contain $n_p = 2$, 4, and 6 parameters, respectively] and three commonly used closures [i.e., the random-phase approximation (RPA),[27] the hypernetted-chain (HNC),[26] and PY[21] closures] for CG systems, and compared our results [including $\beta v(r)$, the minimized RE per chain s_c, the normalized isothermal compressibility κ_T, the interchain internal energy per chain, and the interchain virial pressure P of CG systems at various N] with those of st-based coarse graining.[12]

Due to the absence of the attractive well in $\beta v_{\rm I}(r)$, $\beta v_{\rm I,2}(r)$ is overall smaller than the CG pair potential $\beta v^{\rm st}(r)$ obtained from st-based coarse graining, and $\beta v_{\rm I,1}(r)$ is even much smaller than $\beta v_{\rm I,2}(r)$. $\beta v_{\rm II}(r)$, on the other hand, can well capture the attractive

well of $\beta v^{\rm st}(r)$ and is therefore much closer to it. The deviation between $\beta v^{\rm st}(r)$ and $\beta v(r)$ obtained with the same closure for CG system, $\chi_v^2 \equiv (4\pi/R_{e,0}^3)\int_0^\infty {\rm d}r r^2[\beta v^{\rm st}(r) - \beta v(r)]^2$, in general decreases with increasing n_p and with increasing N. With HNC and PY closures for CG systems, $\beta v(r=0)$ monotonically increase with increasing N as expected, and both $\beta v^{\rm st}(r=0)$ and $\beta v_{\rm II}(r=0)$ scale approximately with $N^{0.18}$. With RPA closure, however, $\beta v(r=0)$ exhibit a maximum around $N=40$, indicating the qualitative failure of RPA closure for CG systems at larger N. Similar to $\tilde{v}^{\rm st}(r) \equiv v^{\rm st}(r)/v^{\rm st}(r=0)$, $\tilde{v}_{\rm II}(r)$ for various N collapse approximately onto the same curve if r is normalized by $R_{e,0}N^{-3/4}$.

s_c provides a quantitative measure of the information loss due to coarse graining, and decreases with increasing N as expected. For st-based coarse graining, $s_{c,\rm HNC}^{\rm st}$ is always smaller than both $s_{c,\rm RPA}^{\rm st}$ and $s_{c,\rm PY}^{\rm st}$, which is qualitatively consistent with the deviation in thermodynamic properties between original and CG systems reported in Paper I.[12] On the other hand, with HNC closure for CG systems (used hereafter) we find that $s_c^{\rm RE} > s_c^{\rm st}$ at the same N, consistent with the fact that st-based coarse graining is equivalent to RE-based coarse graining with unconstrained functional form of $\beta v(r)$ (i.e., in the limit of $n_p \to \infty$), and that $s_c^{\rm RE} - s_c^{\rm st}$ increases with increasing N. Furthermore, $\beta v_{\rm I,2}(r)$ gives much less information loss (thus better coarse-graining performance) than $\beta v_{\rm I,1}(r)$, and $\beta v_{\rm II}(r)$ gives even better coarse-graining performance and is good enough to analytically represent $\beta v^{\rm st}(r)$ in the N-range considered in this paper.

Due to the absence of the attractive well in $\beta v_{\rm I}(r)$, κ_T obtained from RE-based coarse graining using $\beta v_{\rm I,1}(r)$ is significantly larger than $\kappa_T^{\rm st}$ from st-based coarse graining (which is the same as κ_T of the original system), and that using $\beta v_{\rm I,2}(r)$ is closer to $\kappa_T^{\rm st}$ but still overestimates it for small $N \lesssim 10$. Using $\beta v_{\rm II}(r)$ gives better results than using $\beta v_{\rm I}(r)$, although $\kappa_T^{\rm st}$ is somewhat underestimated for small $N \lesssim 10$. On the other hand, using $\beta v_{\rm I,2}(r)$ always underestimates the pressure of the original system, P_m, particularly for $N \lesssim 30$, but gives closer P to P_m than st-based coarse graining for $27 \le N \le 91$. Using $\beta v_{\rm II}(r)$ overestimates P_m for $N \lesssim 30$ and gives better results than using $\beta v_{\rm I,2}(r)$ at small N, but the opposite occurs for $N \ge 36$. Results for the interchain internal energy per chain are similar to those for P. It is therefore not possible to simultaneously

minimize s_c and the deviation in structural and thermodynamic properties (e.g., κ_T and P) from the original system, as these are not equivalent. We have also compared the minimization of χ_v^2 and s_c in Appendix.

Finally, we note that, apart from the approximate closures and the assumption that the interchain total and direct pair correlation functions do not depend on the monomer/segment position along the chain contour in the original/CG system inherent in PRISM theory,[14] the only two assumptions used in our work here are the ideal-chain conformations for the original system and the aforementioned $\omega_{s,s'}(r) = \omega^{ss}_{s,s'}(r)$. These two assumptions can be eliminated by the self-consistent PRISM (SCPRISM) theory,[24,25] which requires single-chain simulations of discrete chain models with nonzero-range interactions but is still much faster than many-chain simulations commonly used in the literature. For RE-based coarse graining, SCPRISM calculations of the original system readily give more accurate results of $\omega^{ss}_{s,s'}(r)$, and those of the CG system give the corresponding $\omega_{s,s'}(r)$, which depend on both the bonding and non-bonded CG pair potentials. RE-based coarse graining using SCPRISM theory, which follows our general strategy proposed in Sec. 2.1, will be reported in a future publication.

Acknowledgement

Financial support for this work was provided by the U.S. Department of Energy, Office of Basic Energy Sciences, Division of Materials Sciences and Engineering under Award No. DE-FG02-07ER46448.

Appendix: Relation between RE minimization and least-squares fitting of CG potential

Here we elucidate the relation between minimization of RE and the least-squares fitting of $\beta v(r)$ to the CG pair potential $\beta v^{\rm st}(r)$ obtained from structure-based (st-based) coarse graining. The least-squares fitting minimizes $\chi_v^2 \equiv (4\pi/R_{e,0}^3)\int_0^\infty {\rm d}r r^2[\beta v^{\rm st}(r) - \beta v(r;\boldsymbol{\lambda})]^2$

with respect to the parameters $\boldsymbol{\lambda} \equiv \{\lambda_j\}$ $(j = 1, \ldots, n_p)$, which is equivalent to solving $\partial\chi_v^2/\partial\lambda_j = 0$, i.e.,

$$\int_0^\infty \mathrm{d}qq^2[\hat{v}^{\mathrm{st}}(q) - \hat{v}(q;\boldsymbol{\lambda})]\hat{v}_j'(q;\boldsymbol{\lambda}) = 0, \tag{20}$$

where $v_j'(r;\boldsymbol{\lambda}) \equiv \partial v(r;\boldsymbol{\lambda})/\partial\lambda_j$ and $\hat{v}_j'(q;\boldsymbol{\lambda})$ denotes its 3D Fourier transform.

On the other hand, minimizing RE (i.e., Eq. (8)) is equivalent to

$$\int_0^\infty \mathrm{d}qq^2[\hat{h}^{ss}(q) - \hat{h}(q;\boldsymbol{\lambda})]\hat{v}_j'(q;\boldsymbol{\lambda}) = 0, \tag{21}$$

where $\hat{h}^{ss}(q;\boldsymbol{\lambda})$ is obtained from st-based coarse graining and $\hat{h}(q;\boldsymbol{\lambda})$ from solving the CG system at $\boldsymbol{\lambda}$ using PRISM theory with a closure. From PRISM equation (i.e., Eq. (9)), we have $\hat{h} = N^2\hat{\omega}^2\hat{c}/(1 - \rho_c N^2\hat{\omega}\hat{c})$, which still holds when $\hat{h}$ and $\hat{c}$ are replaced by $\hat{h}^{ss}$ and $\hat{c}^{ss}$, respectively, with $\hat{\omega} = \hat{\omega}^{ss}$. Eq. (21) then becomes

$$\int_0^\infty \mathrm{d}qq^2[\hat{c}^{ss}(q) - \hat{c}(q;\boldsymbol{\lambda})]S^{\mathrm{st}}(q)S(q;\boldsymbol{\lambda})\hat{v}_j'(q;\boldsymbol{\lambda}) = 0, \tag{22}$$

where $S^{\mathrm{st}} \equiv (1/\hat{\omega} - \rho_c N^2\hat{c}^{ss})^{-1}$ and $S \equiv (1/\hat{\omega} - \rho_c N^2\hat{c})^{-1}$ are the structure factor of CG systems obtained from st- and RE-based coarse graining, respectively.

If RPA closure is used for CG systems, i.e., $c^{ss}(r) = -\beta v^{\mathrm{st}}(r)$ and $c(r) = -\beta v(r;\boldsymbol{\lambda})$, Eq. (22) becomes

$$\int_0^\infty \mathrm{d}qq^2[\hat{v}^{\mathrm{st}}(q) - \hat{v}(q;\boldsymbol{\lambda})]S^{\mathrm{st}}(q)S(q;\boldsymbol{\lambda})\hat{v}_j'(q;\boldsymbol{\lambda}) = 0. \tag{23}$$

Comparing Eq. (23) to Eq. (20), we see that RE minimization with RPA closure for CG systems is equivalent to a specifically weighted (by $S^{\mathrm{st}}(q)S(q;\boldsymbol{\lambda})$) least-squares fitting of $\beta v(r)$ to $\beta v^{\mathrm{st}}(r)$.

With HNC closure, i.e., $c^{ss}(r) = -\beta v^{\mathrm{st}}(r) + h^{ss}(r) - \ln[1 + h^{ss}(r)] = -\beta v^{\mathrm{st}}(r) + \Delta h^{ss}(r)$ and $c(r) = -\beta v(r;\boldsymbol{\lambda}) + h(r;\boldsymbol{\lambda}) - \ln[1 + h(r;\boldsymbol{\lambda})] = -\beta v(r;\boldsymbol{\lambda}) + \Delta h(r;\boldsymbol{\lambda})$, where $\Delta h^{ss}(r) \equiv h^{ss}(r) - \ln[1 + h^{ss}(r)] \sim O((h^{ss})^2)$ and $\Delta h(r;\boldsymbol{\lambda}) \equiv h(r;\boldsymbol{\lambda}) - \ln[1 + h(r;\boldsymbol{\lambda})] \sim O(h^2)$,

Eq. (22) becomes

$$\int_0^\infty \mathrm{d}qq^2 \left\{\beta\left[\hat{v}^{\mathrm{st}}(q) - \hat{v}(q;\boldsymbol{\lambda})\right] - \left[\widehat{\Delta h}^{ss}(q) - \widehat{\Delta h}(q;\boldsymbol{\lambda})\right]\right\} S^{\mathrm{st}}(q)S(q;\boldsymbol{\lambda})\hat{v}'_j(q;\boldsymbol{\lambda}) = 0, \quad (24)$$

which can be compared to Eq. (20).

It is therefore clear that, in general, least-squares fitting of $\beta v(r)$ to $\beta v^{\mathrm{st}}(r)$ is not equivalent to RE minimization and gives higher RE (thus worse coarse-graining performance) than the latter.

References

[1] See, for example, J. Baschnagel, K. Binder, P. Doruker, A. A. Gusev, O. Hahn, K. Kremer, W. L. Mattice, F. Muller-Plathe, M. Murat, W. Paul, S. Santos, U. W. Suter and V. Tries, *Adv. Polym. Sci.*, 2000, **152**, 41; F. Muller-Plathe, *Chem. Phys. Chem.*, 2002, **3**, 754; F. Muller-Plathe, *Soft Mater*, 2003, **1**, 1; C. Peter and K. Kremer, *Soft Matter*, 2009, **5**, 4357; C. Peter and K. Kremer, *Faraday Discuss.*, 2010, **144**, 9; E. Brini, E. A. Algaer, P. Ganguly, C. Li, F. Rodriguez-Ropero and N. F. A. van der Vegt, *Soft Matter*, 2013, **9**, 2108; Y. Li, B. C. Abberton, M. Kroger and W. K. Liu, *Polymers*, 2013, **5**, 751; W. G. Noid, *J. Chem. Phys.*, 2013, **139**, 090901; M. G. Saunders and G. A. Voth, *Annu. Rev. Biophys.*, 2013, **42**, 73; R. Potestio, C. Peter and K. Kremer, *Entropy*, 2014, **16**, 4199; and references therein.

[2] F. Ercolessi and J. B. Adams, *Europhys. Lett.*, 1994, **26**, 583.

[3] A. P. Lyubartsev and A. Laaksonen, *Phys. Rev. E*, 1995, **52**, 3730.

[4] A. K. Soper, *Chem. Phys.*, 1996, **202**, 295.

[5] D. Reith, M. Putz and F. Muller-Plathe, *J. Comput. Chem.*, 2003, **24**, 1624.

[6] S. Izvekov and G. A. Voth, *J. Phys. Chem. B*, 2005, **109**, 2469.

[7] S. Izvekov and G. A. Voth, *J. Chem. Phys.*, 2005, **123**, 134105.

[8] W. G. Noid, J. W. Chu, G. S. Ayton, V. Krishna, S. Izvekov, G. A. Voth, A. Das and H. C. Andersen, *J. Chem. Phys.*, 2008, **128**, 244114.

[9] M. S. Shell, *J. Chem. Phys.*, 2008, **129**, 144108.

[10] A. P. Lyubartsev, A. Mirzoev, L. J. Chen and A. Laaksonen, *Faraday Discuss.*, 2010, **144**, 43.

[11] A. J. Clark and M. G. Guenza, *J. Chem. Phys.*, 2010, **132**, 044902.

[12] D. Yang and Q. Wang, *J. Chem. Phys.*, 2015, **142**, 054905.

[13] D. Chandler and H. C. Andersen, *J. Chem. Phys.*, 1972, **57**, 1930.

[14] K. S. Schweizer and J. G. Curro, *Phys. Rev. Lett.*, 1987, **58**, 246; J. G. Curro and K. S. Schweizer, *Macromolecules*, 1987, **20**, 1928.

[15] E. F. David and K. S. Schweizer, *J. Chem. Phys.*, 1994, **100**, 7767; *ibid.*, 1994, **100**, 7784.

[16] A. A. Louis, *J. Phys.: Condens. Matter*, 2002, **14**, 9187.

[17] M. E. Johnson, T. Head-Gordon and A. A. Louis, *J. Chem. Phys.*, 2007, **126**, 144509.

[18] A. Chaimovich and M. S. Shell, *Phys. Rev. E*, 2010, **81**, 060104.

[19] A. Chaimovich and M. S. Shell, *J. Chem. Phys.*, 2011, **134**, 094112.

[20] K. S. Schweizer and J. G. Curro, *Chem. Phys.*, 1990, **149**, 105.

[21] J. K. Percus and G. J. Yevick, *Phys. Rev.*, 1958, **110**, 1.

[22] G. H. Fredrickson, E. Helfand, F. S. Bates, and L. Leibler, *Chem. Phys.*, 1989, **51**, 13.

[23] In our definition of RE, we do not consider the mapping entropy defined in Ref. [9], which does not depend on CG potential.

[24] K. S. Schweizer, K. G. Honnell and J. G. Curro, *J. Chem. Phys.*, 1992, **96**, 3211.

[25] D. R. Heine, G. S. Grest and J. G. Curro, *Adv. Polym. Sci.*, 2005, **173**, 209.

[26] J. P. Hansen and I. R. McDonald, *Theory of Simple Liquids*, Academic Press, London, 1976.

[27] A. A. Louis, P. G. Bolhuis and J. P. Hansen, *Phys. Rev. E*, 2000, **62**, 7961.

[28] R. B. Thompson, K. Ø. Rasmussen and T. Lookman, *J. Chem. Phys.*, 2004, **120**, 31.

[29] M. W. Matsen, *Eur. Phys. J. E*, 2009, **30**, 361.

[30] http://www.fftw.org.

[31] W. H. Press, S. A. Teukolsky, W. T. Vetterling and B. P. Flannery, *Numerical Recipes in C*, Cambridge University Press, New York, 2nd Ed., 1992.

[32] A. J. Clark, J. McCarty, I. Y. Lyubimov and M. G. Guenza, *Phys. Rev. Lett.*, 2012, **109**, 168301.

List of Figures

Figure 1. (a) Non-bonded CG pair potentials $\beta v(r)$, (b) $\tilde{r}^2\beta v$, and (c) $\tilde{r}^3 \mathrm{d}\beta v/\mathrm{d}\tilde{r}$ obtained from st- and RE-based coarse graining at various N (number of CG segments per chain) with various parameterization in the latter, where $\tilde{r} \equiv N^{3/4} r/R_{e,0}$ with $R_{e,0}$ denoting the root-mean-square end-to-end distance of an ideal chain in the original system. (d) Deviation χ_v^2 between $\beta v^{\mathrm{st}}(r)$ obtained from st-based coarse graining and $\beta v(r)$ from RE-based coarse graining with various parameterization. (e) $\beta v(r = 0)$ obtained from st- and RE-based coarse graining with various closures for CG systems and parameterization in the latter. HNC closure for CG systems is used in Parts (a)$\sim$(d), and $\bar{\mathcal{N}} = 10^4$ in all cases.

Figure 2. (a) Normalized CG potential $\tilde{v}_{\mathrm{II}}(r)$ obtained from RE-based coarse graining at various N. (b) Corresponding parameters of $\tilde{v}_{\mathrm{II}}(r)$. HNC closure for CG systems is used and $\bar{\mathcal{N}} = 10^4$.

Figure 3. (a) Relative entropy per chain s_c^{st} for st-based coarse graining with various closures for CG systems. (b) Difference in s_c between RE- and st-based coarse graining with various parameterization in the former and HNC closure for CG systems. $\bar{\mathcal{N}} = 10^4$.

Figure 4. Comparisons of (a) the normalized isothermal compressibility κ_T and (b) the interchain virial pressure P of CG systems obtained from RE-based coarse graining with various parameterization, those from st-based coarse graining, and those of the original system (represented by the black horizontal line). HNC closure for CG systems is used and $\bar{\mathcal{N}} = 10^4$.

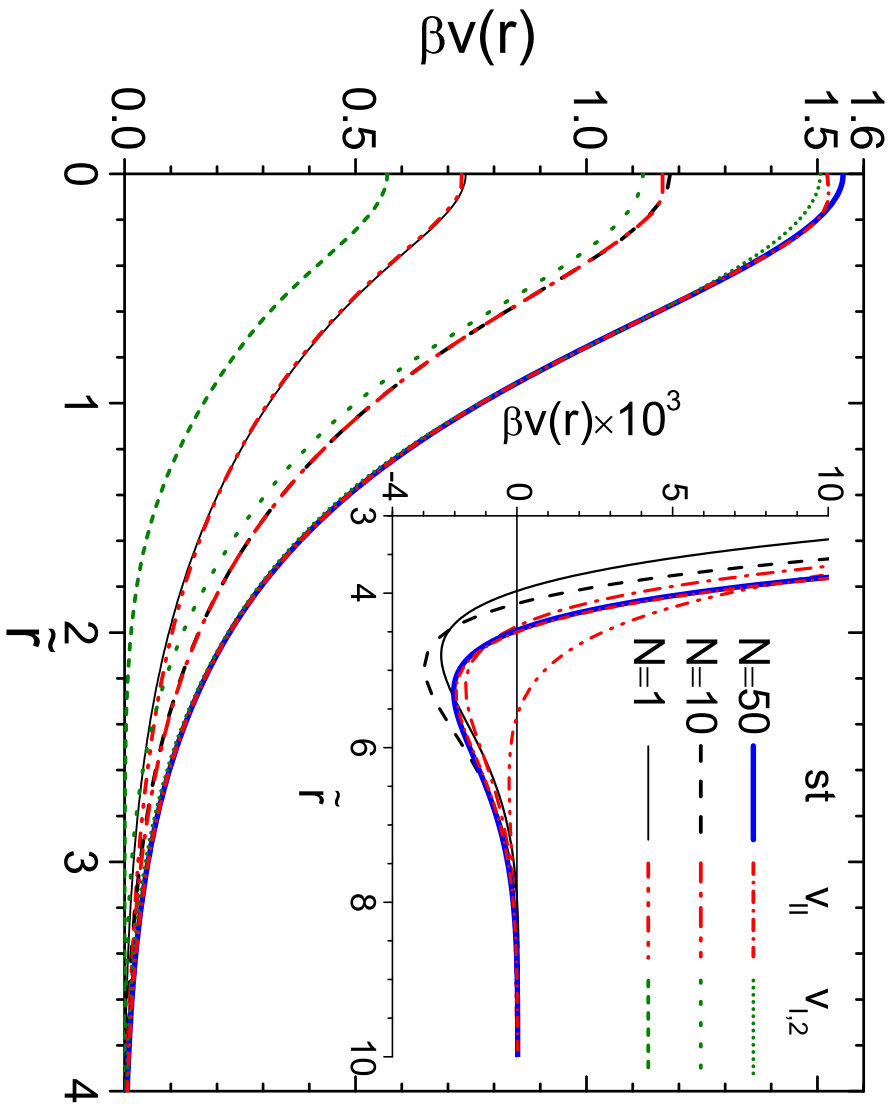

Figure 1: (a)

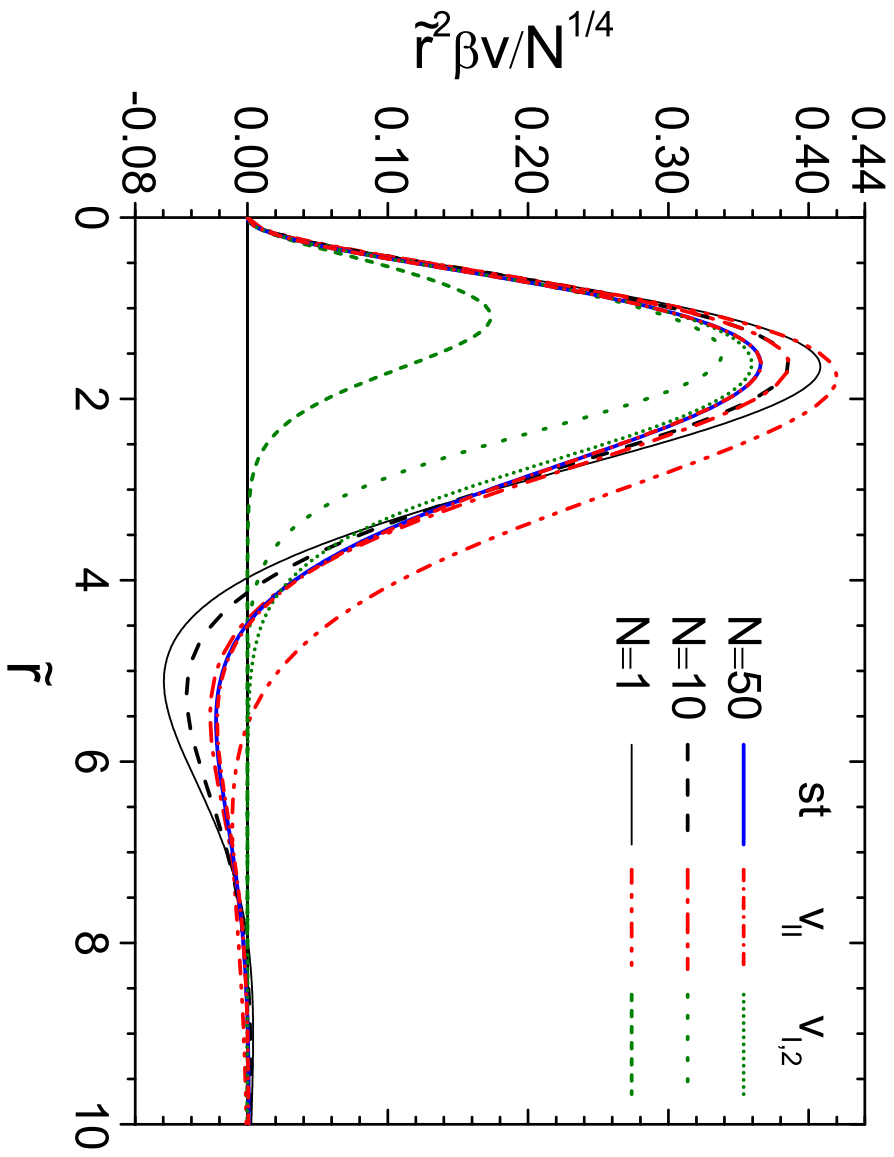

Figure 1: (b)

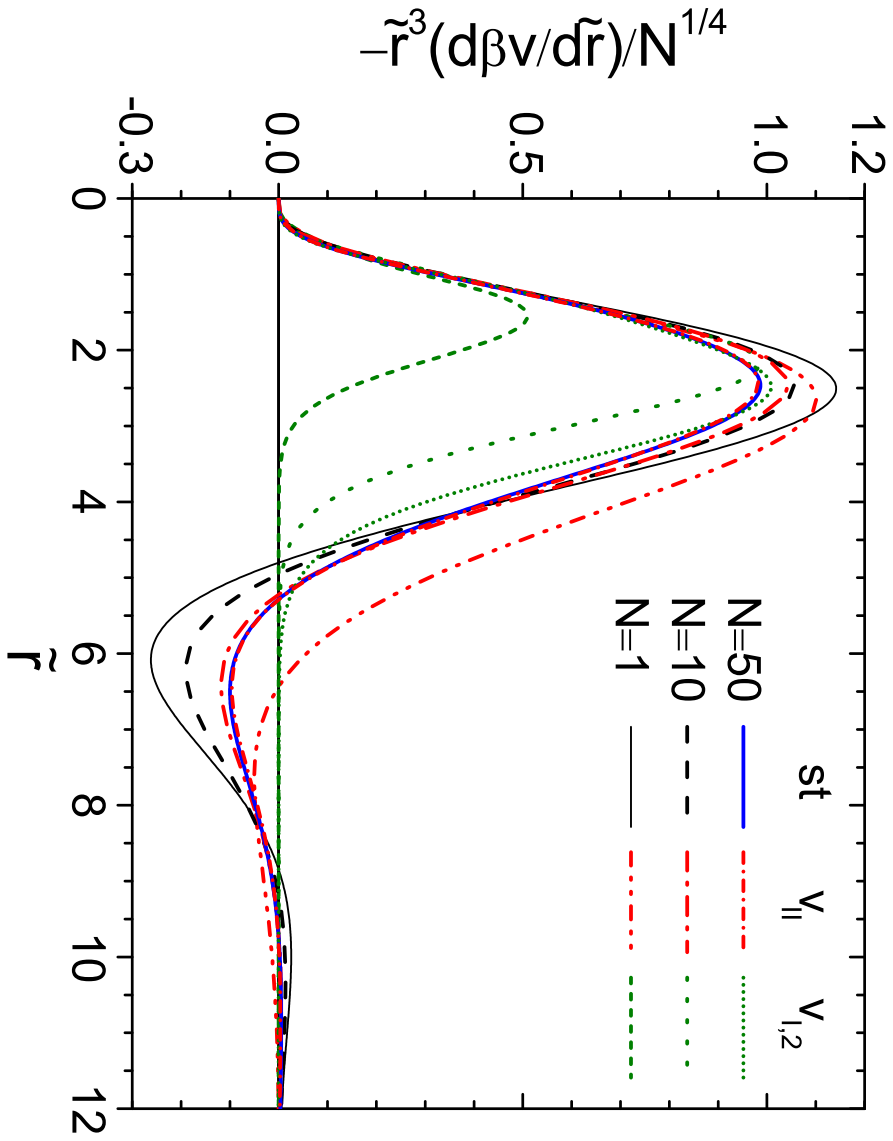

Figure 1: (c)

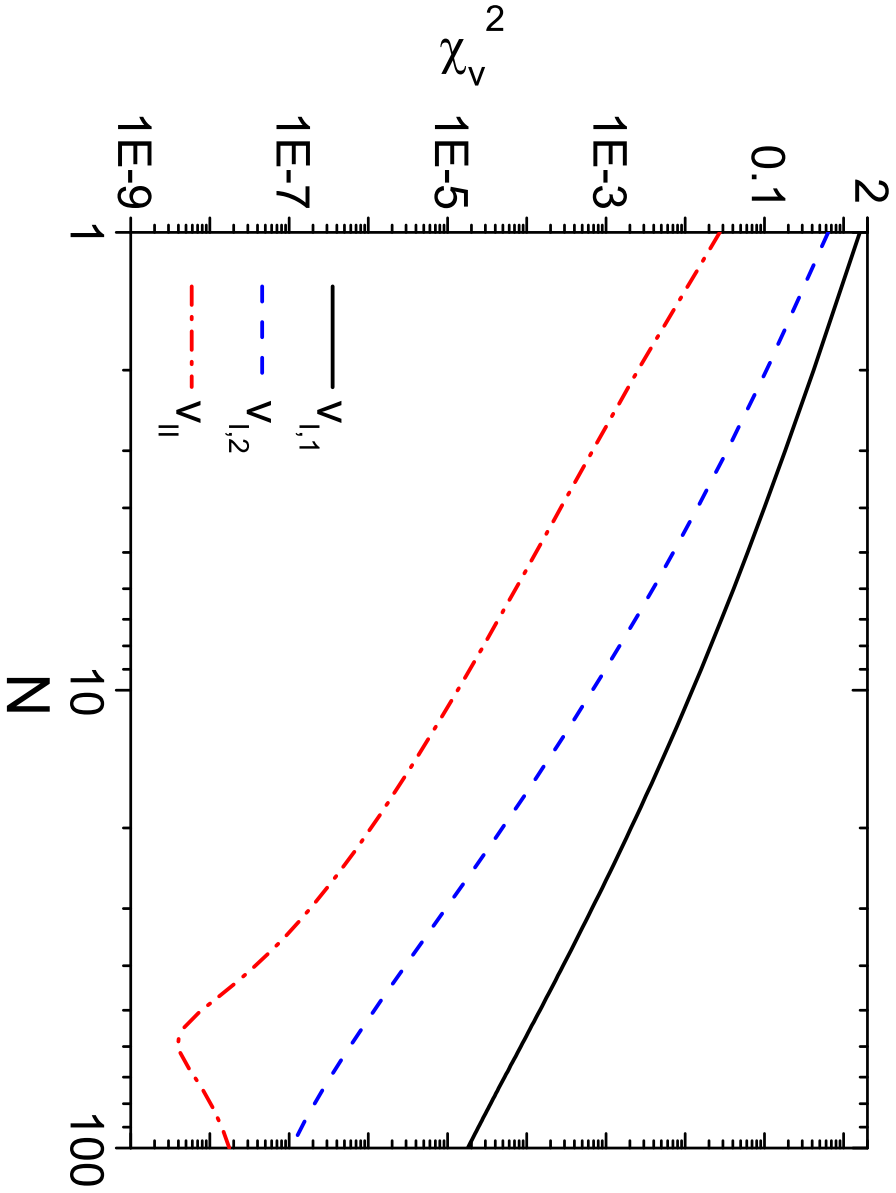

Figure 1: (d)

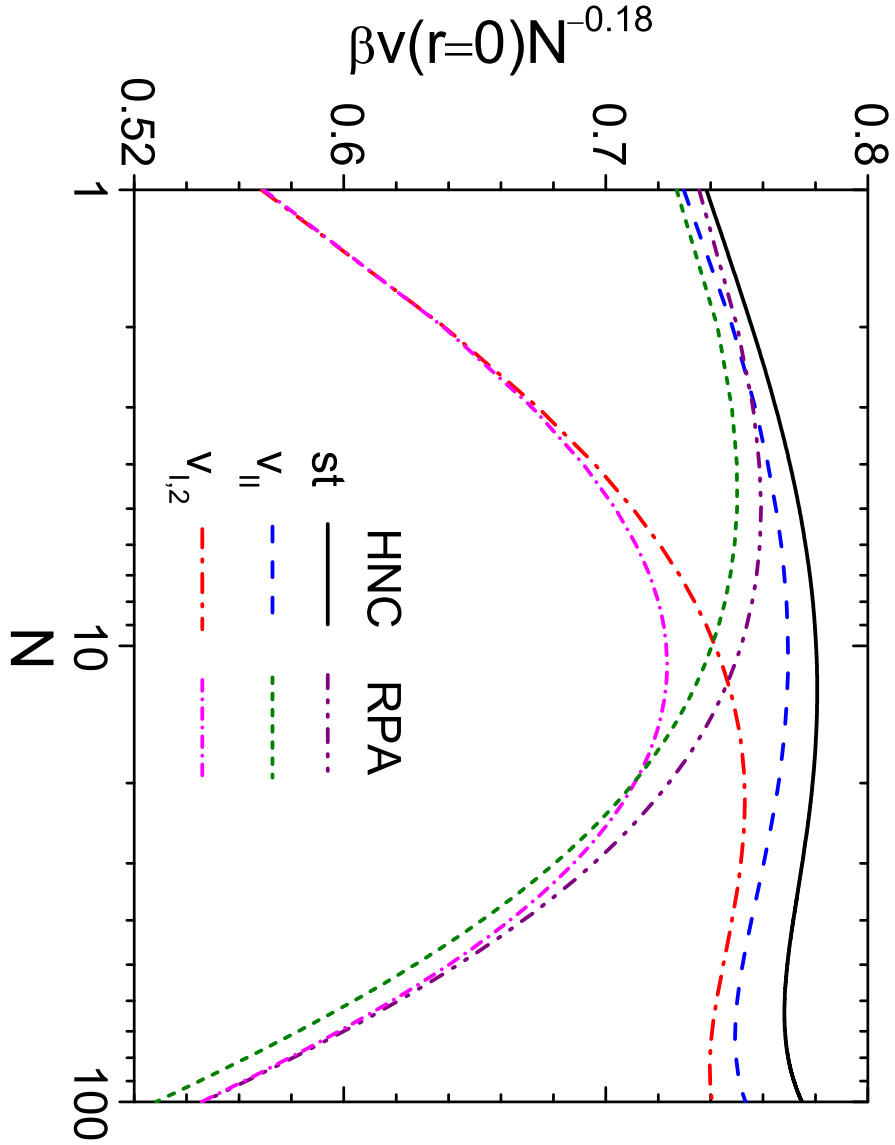

Figure 1: (e)

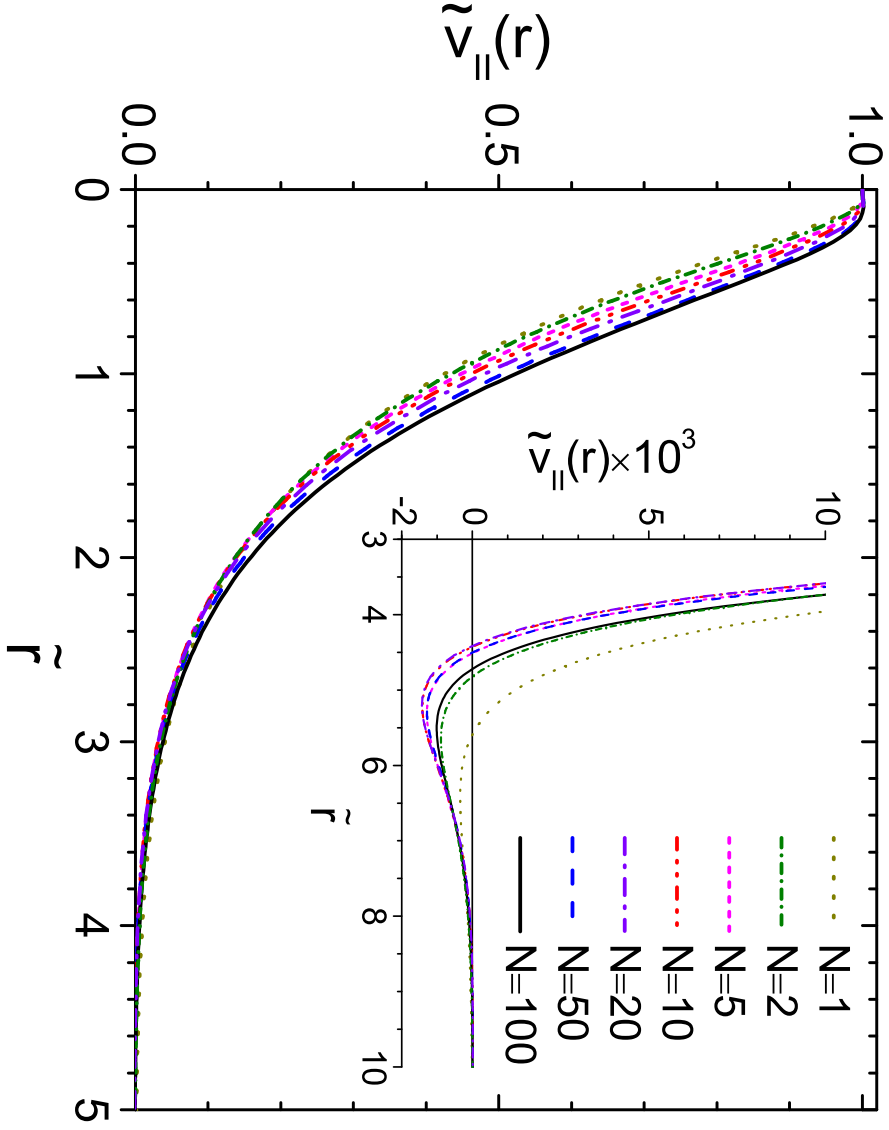

Figure 2: (a)

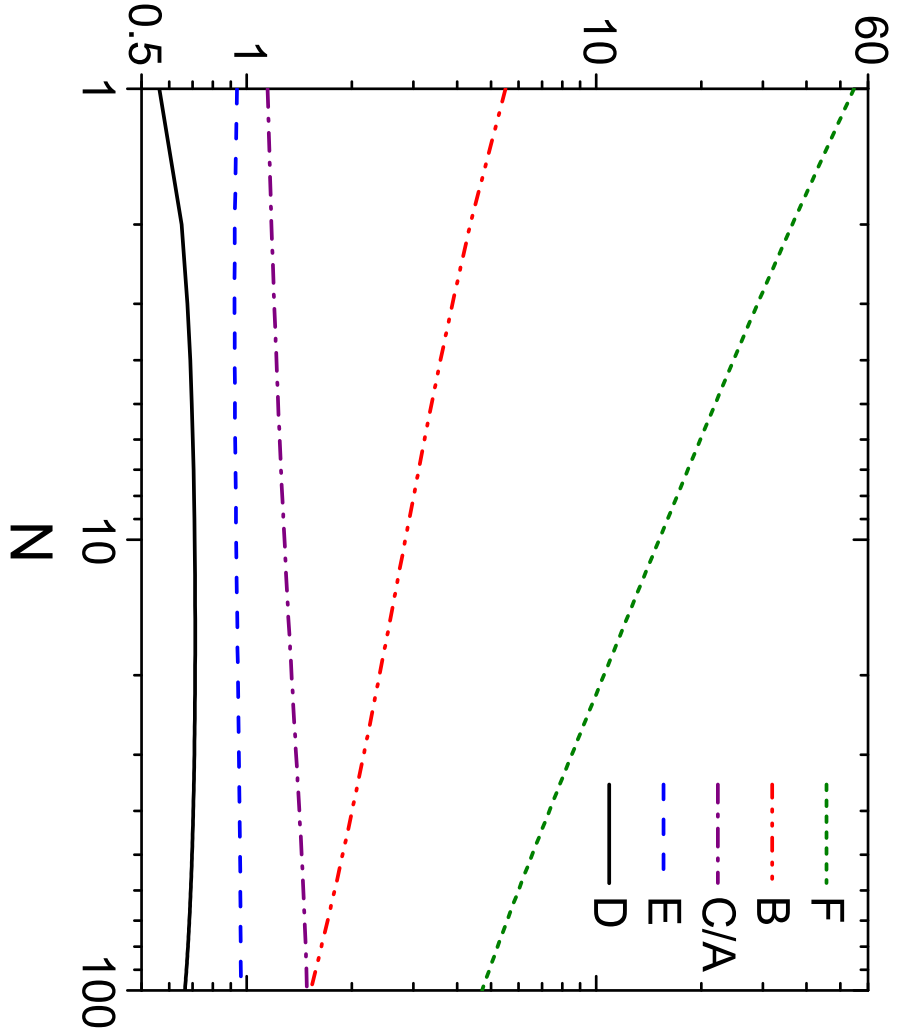

Figure 2: (b)

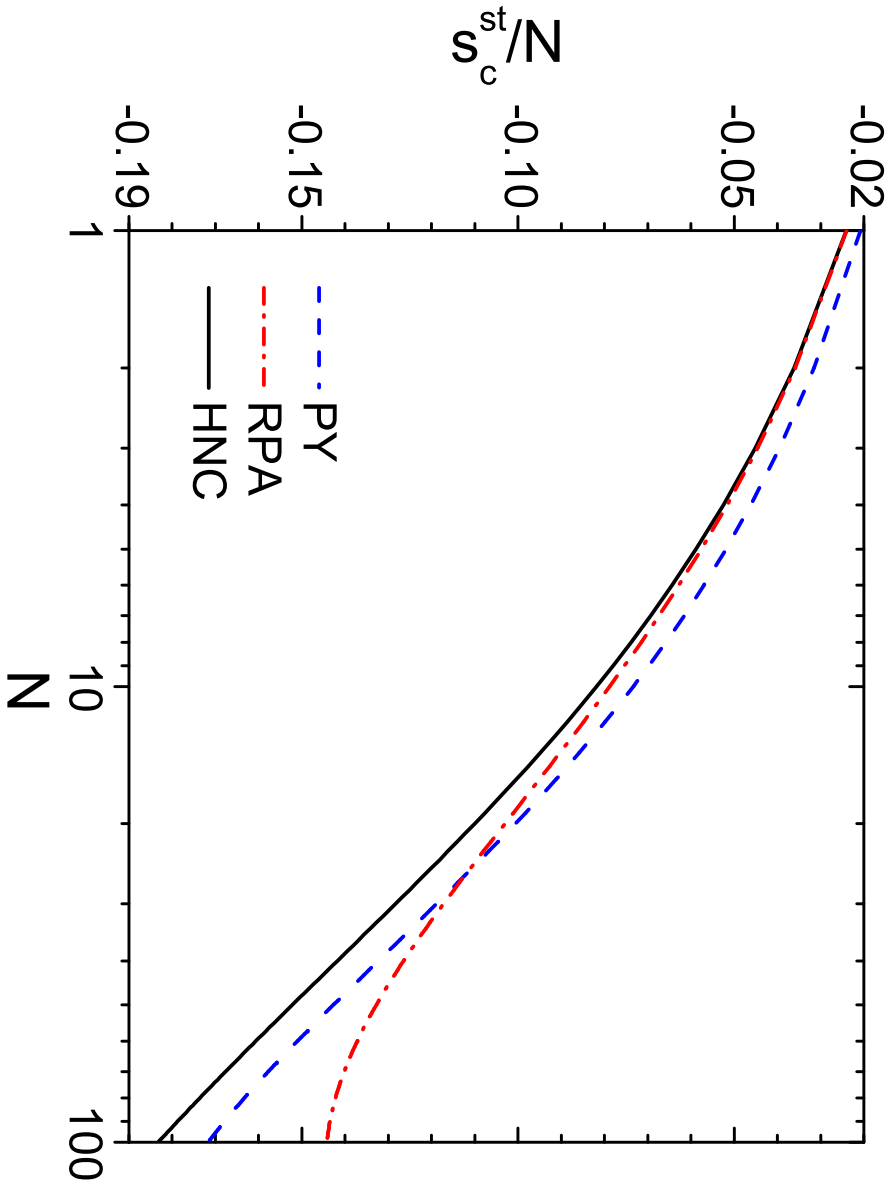

Figure 3: (a)

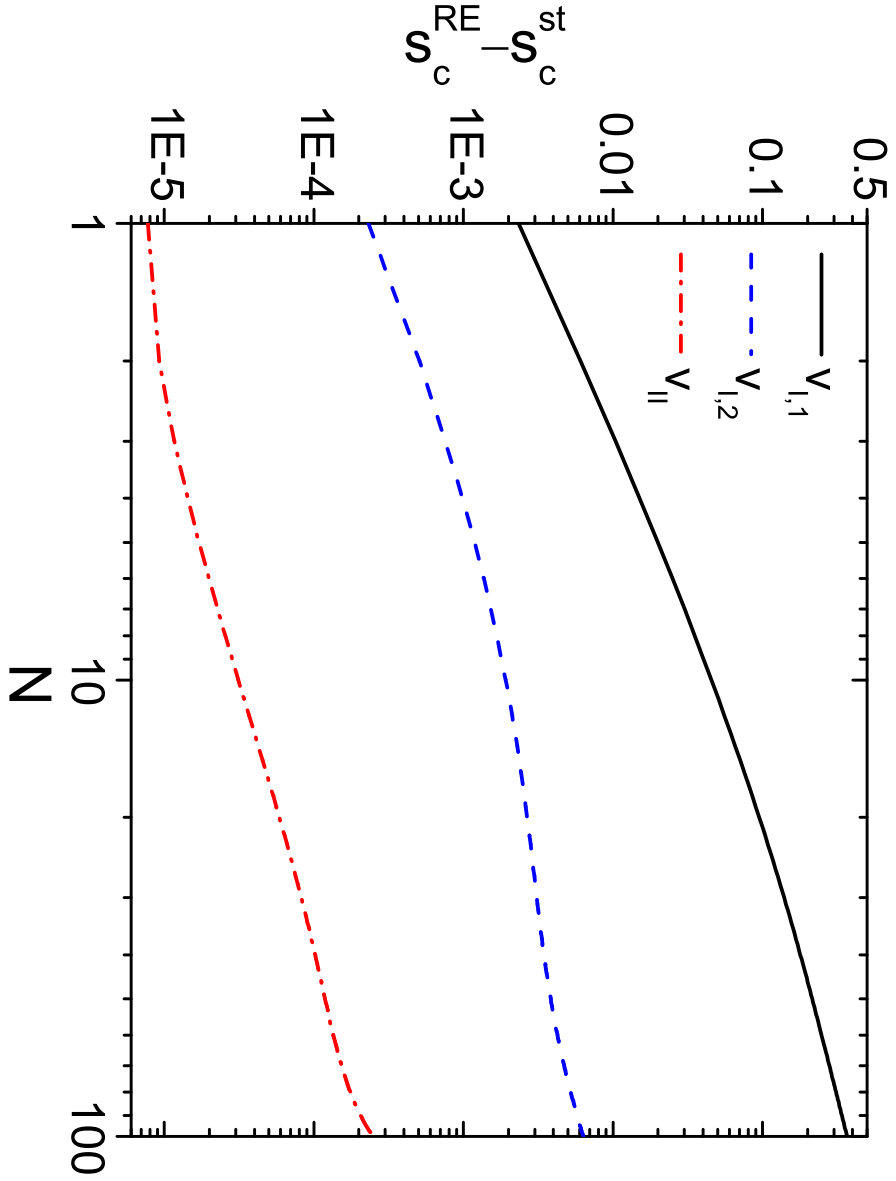

Figure 3: (b)

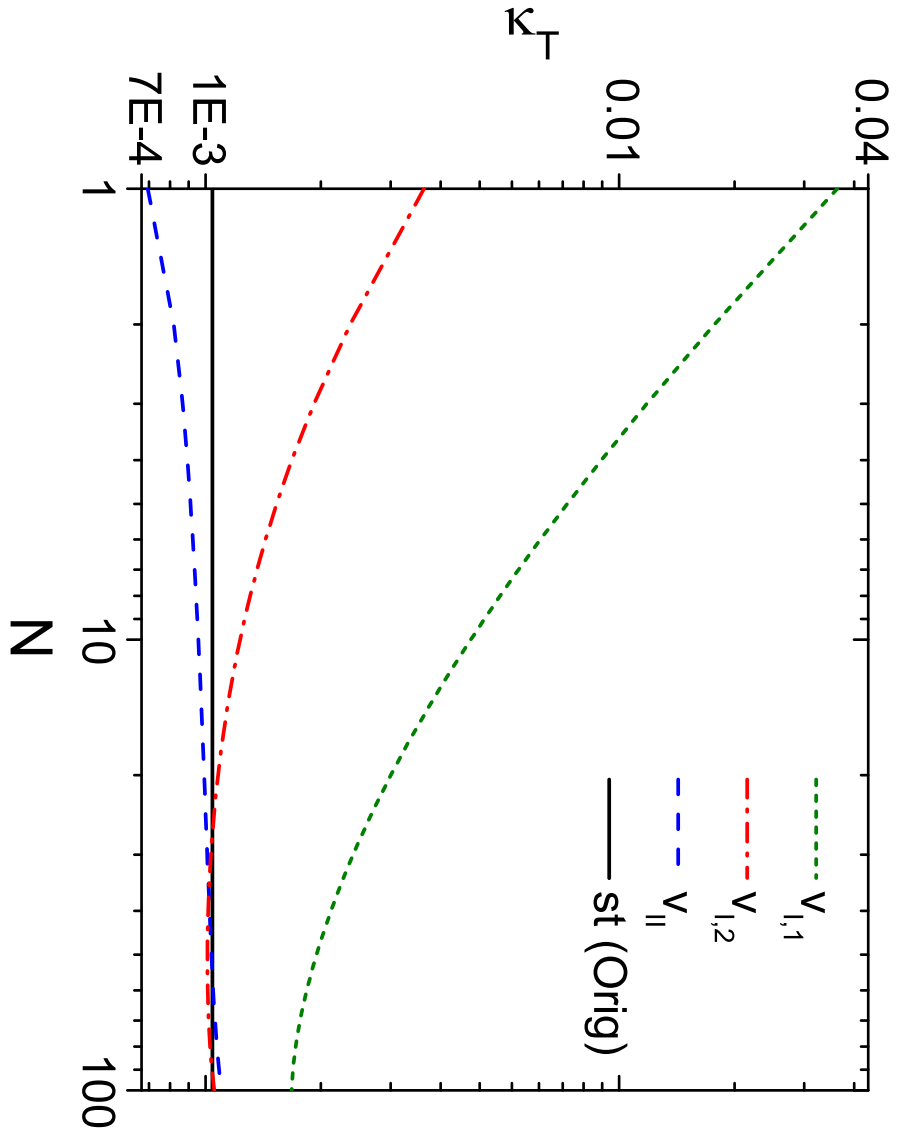

Figure 4: (a)

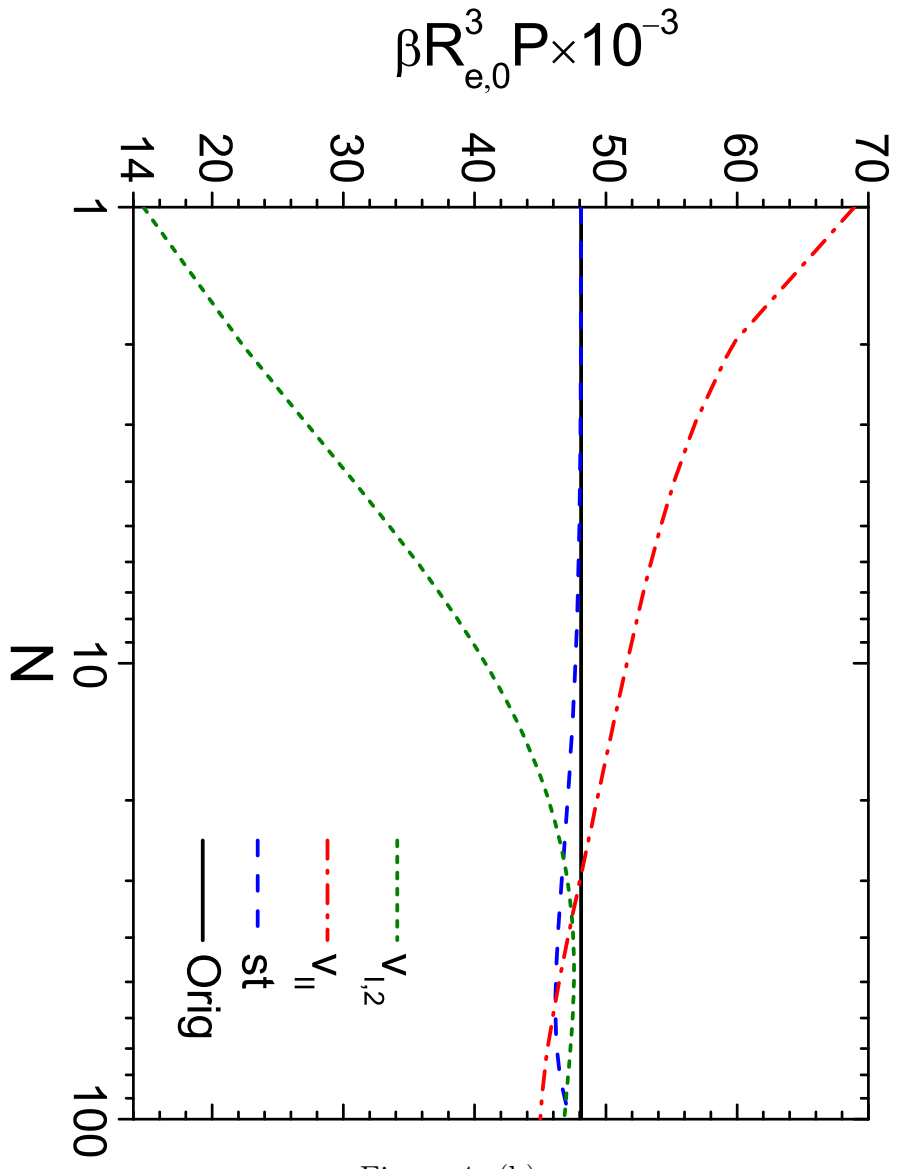

Figure 4: (b)